ELSEVIER
Available online at www.sciencedirect.com
ScienceDirect
Journal of Computational and Applied Mathematics 220 (2008) 215–225
JOURNAL OF COMPUTATIONAL AND APPLIED MATHEMATICS
www.elsevier.com/locate/cam

Mathematical modeling of time fractional reaction–diffusion systems

V. Gafiychuk[a, b, c, *], B. Datsko[c], V. Meleshko[c]

[a] *Institute of Computer Modeling, Krakow University of Technology, 24 Warszawska Street, Krakow 31155, Poland*
[b] *Physics Department, New York City College of Technology, CUNY, 300 Jay Street, NY, NY 11201, USA*
[c] *Institute of Applied Problem of Mechanics and Mathematics, National Academy of Sciences of Ukraine, Naukova Street 3 B, Lviv 79053, Ukraine*

Received 28 November 2006; received in revised form 7 August 2007

Abstract

We study a fractional reaction–diffusion system with two types of variables: activator and inhibitor. The interactions between components are modeled by cubical nonlinearity. Linearization of the system around the homogeneous state provides information about the stability of the solutions which is quite different from linear stability analysis of the regular system with integer derivatives. It is shown that by combining the fractional derivatives index with the ratio of characteristic times, it is possible to find the marginal value of the index where the oscillatory instability arises. The increase of the value of fractional derivative index leads to the time periodic solutions. The domains of existing periodic solutions for different parameters of the problem are obtained. A computer simulation of the corresponding nonlinear fractional ordinary differential equations is presented. For the fractional reaction–diffusion systems it is established that there exists a set of stable spatio-temporal structures of the one-dimensional system under the Neumann and periodic boundary conditions. The characteristic features of these solutions consist of the transformation of the steady-state dissipative structures to homogeneous oscillations or space temporary structures at a certain value of fractional index and the ratio of characteristic times of system.

Keywords: Reaction–diffusion system; Fractional differential equations; Oscillations; Dissipative structures; Pattern formation; Spatio-temporal structures

1. Introduction

Reaction–diffusion systems (RDS) have been extensively used in the study of self-organization phenomena in physics, biology, chemistry, ecology, etc. (see, for example, [23,3,21,13,4,5,16,9,30,22]). The main result obtained from these systems is that nonlinear phenomena include diversity of stationary and spatio-temporary dissipative patterns, oscillations, different types of waves, excitability, bistability, etc. The mechanism of the formation of such type of nonlinear phenomena and the conditions of their emergence have been extensively studied during the last couple decades.

In the recent years, there has been a great deal of interest in fractional reaction–diffusion (FRD) systems [10–12,31,7,8, 29,38,33] which from one side exhibit self-organization phenomena and from the other side introduce a new parameter

* Corresponding author. Institute of Computer Modeling, Krakow University of Technology, 24 Warszawska Street, Krakow 31155, Poland.
E-mail address: vagaf@yahoo.com (V. Gafiychuk).

0377-0427/$ - see front matter
doi:10.1016/j.cam.2007.08.011

to these systems, which is a fractional derivative index, and it gives a great degree of freedom for diversity of self-organization phenomena and new nonlinear effects [10,11,27,32,15] depending on the order of time-space fractional derivatives. Following these seminal ideas of understanding nonlinear phenomena by different orders of the derivatives we would like to put your attention that time fractional derivatives change also the solutions we usually get in standard RDS. Analyzing structures in FRD systems evolve, both from the point of view of the qualitative analysis and from the computer simulation. Our particular interest is the analysis of the specific nonlinear system of FRD equations. We consider a very well-known example of the RDS with cubical nonlinearity [21,13,16] which probably is the simplest one used in RD systems modeling

$$\tau_1 \frac{\partial^\alpha n_1(x,t)}{\partial t^\alpha} = l^2 \nabla^2 n_1(x,t) + n_1 - n_1^3/3 - n_2, \tag{1}$$

$$\tau_2 \frac{\partial^\alpha n_2(x,t)}{\partial t^\alpha} = L^2 \nabla^2 n_2(x,t) - n_2 + \beta n_1 + \mathscr{A} \tag{2}$$

subject to

(i) Neumann:

$$\mathrm{d}n_i/\mathrm{d}x|_{x=0} = \mathrm{d}n_i/\mathrm{d}x|_{x=l_x} = 0, \quad i = 1, 2 \tag{3}$$

or

(ii) periodic:

$$n_i(t,0) = n_i(t,l_x), \quad \mathrm{d}n_i/\mathrm{d}x|_{x=0} = \mathrm{d}n_i/\mathrm{d}x|_{x=l_x}, \quad i = 1, 2 \tag{4}$$

boundary conditions and with the certain initial conditions. Here $x : 0 \leqslant x \leqslant l_x$; $(x,t) \in \mathbb{R} \times \mathbb{R}_+$; $\nabla^2 = \partial^2/\partial x^2$; $n_1(x,t)$, $n_2(x,t) \in \mathbb{R}$: activator and inhibitor variables correspondingly; $\tau_1, \tau_2, l, L, \in \mathbb{R}$: characteristic times and lengths of the system; $\mathscr{A} \in \mathbb{R}$ is an external parameter.

Fractional derivatives $\partial^\alpha n(x,t)/\partial t^\alpha$ on the left-hand side of Eqs. (1), (2) instead of standard time derivatives are the Caputo fractional derivatives in time of the order $0 < \alpha < 2$ and are represented as [28,26]

$$\frac{\partial^\alpha}{\partial t^\alpha} n(t) := \frac{1}{\Gamma(m-\alpha)} \int_0^t \frac{n^{(m)}(\tau)}{(t-\tau)^{\alpha+1-m}} \, \mathrm{d}\tau, \quad m - 1 < \alpha < m, \ \ m \in N.$$

It should be noted that Eqs. (1), (2) at $\alpha = 1$ correspond to standard RDS. Analyzing the influence of the parameter α we notice that the system describes a relaxation process ("sub-diffusion") when $0 < \alpha < 1$ [20,36]. If $1 < \alpha < 2$, an oscillation process ("super-diffusion") may occur [17,14,2,1]. In other words, in the case $1 < \alpha < 2$ we have "sub-oscillating" diffusion and equations describe properties that are similar to hyperbolic fractional RDS [19]. Despite the fact that for $1 < \alpha < 2$ we do not have a classical super-diffusion that is revealed for space fractional derivatives [27], we call this process as a time "super-diffusive". This is analogous to the definition taken from diffusion process with time-dependent mean square displacement $\sim t^\alpha$, where $\alpha > 1$.

2. Linear stability analysis

Stability of the steady-state constant solutions of system (1), (2) correspond to homogeneous equilibrium state

$$W = n_1 - n_1^3/3 - n_2 = 0, \quad Q = -n_2 + \beta n_1 + \mathscr{A} = 0 \tag{5}$$

can be analyzed by linearization of the system nearby this solution. In this case system (1), (2) can be transformed to linear system at equilibrium point (5) and linearized around this equilibrium state. As a result we have

$$\frac{\partial^\alpha \mathbf{u}(x,t)}{\partial t^\alpha} = \widehat{F}(u)\mathbf{u}(x,t), \tag{6}$$

where

$$\mathbf{u}(x,t) = \begin{pmatrix} \Delta n_1(x,t) \\ \Delta n_2(x,t) \end{pmatrix}, \quad \widehat{F}(u) = \begin{pmatrix} (l^2\nabla^2 + a_{11})/\tau_1 & a_{12}/\tau_1 \\ a_{21}/\tau_2 & (L^2\nabla^2 + a_{22})/\tau_2 \end{pmatrix}$$

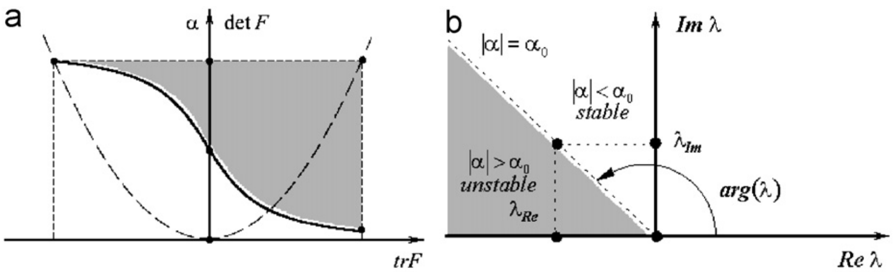

Fig. 1. Schematic view of the marginal curve of α (solid line), describing fixed points for two-dimensional vector field (a), the position of eigenvalue λ corresponding to marginal value of α in the coordinate system (Re λ, Im λ) (b). Shaded domains correspond to instability region.

is a Frechet derivative with respect to $\mathbf{u}(x,t)$, $a_{11}=W'_{n_1}$, $a_{12}=W'_{n_2}$, $a_{21}=Q'_{n_1}$, $a_{22}=Q'_{n_2}$ (all derivatives are taken at homogeneous equilibrium states (5)). By substituting the solution in the form $\mathbf{u}(x,t)=\begin{pmatrix}\Delta n_1(t)\\ \Delta n_2(t)\end{pmatrix}\cos kx$, $k=(\pi/l_x)j$, $j=1,2,\ldots$ into FRD system (6) we can get the system of linear ordinary differential equations (6) with the matrix F determined by the operator $\widehat{F}$.

For analyzing stability conditions of Eqs. (1), (2) let us use simple linear transformation which can convert this linear system (6) to a diagonal form

$$\frac{\mathrm{d}^{\alpha}\boldsymbol{\eta}(t)}{\mathrm{d}t^{\alpha}}=C\boldsymbol{\eta}(t), \tag{7}$$

where C is a diagonal matrix for F: $C=P^{-1}FP=\begin{pmatrix}\lambda_1 & 0\\ 0 & \lambda_2\end{pmatrix}$, eigenvalues $\lambda_{1,2}$ are determined by the characteristic equation of the matrix F, $\lambda_{1,2}=\frac{1}{2}(\operatorname{tr}F\pm\sqrt{\operatorname{tr}^2F-4\det F})$, $\boldsymbol{\eta}(t)=P^{-1}\begin{pmatrix}\Delta n_1(t)\\ \Delta n_2(t)\end{pmatrix}$, P is the matrix of eigenvectors of matrix F.

In this case, the solution of the vector equation (7) is given by Mittag–Leffler functions [28,26,24,35]

$$\Delta n_i(t)=\sum_{k=0}^{\infty}\frac{(\lambda_i t^{\alpha})^k}{\Gamma(k\alpha+1)}\Delta n_i(0)=E_{\alpha}(\lambda_i t^{\alpha})\Delta n_i(0),\quad i=1,2. \tag{8}$$

Using the result obtained in the papers [8,18], we can conclude that if for any of the roots

$$|\operatorname{Arg}(\lambda_i)|<\alpha\pi/2 \tag{9}$$

the solution has an increasing function component then the system is asymptotically unstable.

Analyzing the roots of the characteristic equations, we can see that at $4\det F-\operatorname{tr}^2F>0$ eigenvalues are complex and can be represented as

$$\lambda_{1,2}=\tfrac{1}{2}(\operatorname{tr}F\pm \mathrm{i}\sqrt{4\det F-\operatorname{tr}^2F})\equiv\lambda_{\mathrm{Re}}\pm \mathrm{i}\lambda_{\mathrm{Im}}.$$

The roots $\lambda_{1,2}$ are complex inside the parabola (Fig. 1(a)) and the fixed points are the spiral source ($\operatorname{tr}F>0$) or spiral sinks ($\operatorname{tr}F<0$). The plot of the marginal value $\alpha:\alpha=\alpha_0=(2/\pi)|\operatorname{Arg}(\lambda_i)|$ which follows from the conditions (9) is given by the formula

$$\alpha_0=\begin{cases}\dfrac{2}{\pi}\arctan\sqrt{4\det F/\operatorname{tr}^2F-1}, & \operatorname{tr}F\geqslant 0,\\[2mm] 2-\dfrac{2}{\pi}\arctan\sqrt{4\det F/\operatorname{tr}^2F-1}, & \operatorname{tr}F\leqslant 0\end{cases} \tag{10}$$

and is presented in the Fig. 1.

Let us analyze the system solution with the help of Fig. 1(a). Consider the parameters which keep the system inside the parabola. It is a well-known fact, that at $\alpha=1$ the domain on the right-hand side of the parabola ($\operatorname{tr}F>0$) is unstable with the existing limit circle, while the domain on the left-hand side ($\operatorname{tr}F<0$) is stable. By crossing the axis $\operatorname{tr}F=0$ the Hopf bifurcation conditions become true.

In the general case of $\alpha : 0<\alpha<2$ for every point inside the parabola there exists a marginal value of α_0 where the system changes its stability. The value of α is a certain bifurcation parameter which switches the stable and unstable state of the system. At lower $\alpha : \alpha<\alpha_0=(2/\pi)|\mathrm{Arg}(\lambda_i)|$ the system has oscillatory modes but they are stable. Increasing the value of $\alpha>\alpha_0=(2/\pi)|\mathrm{Arg}(\lambda_i)|$ leads to instability. As a result, the domain below the curve α_0, as a function of tr F is stable and the domain above the curve is unstable.

The plot of the roots, describing the mechanism of the system instability, can be understood from Fig. 1(b) where the case $\alpha_0>1$ is described. In fact, having complex number λ_i with Re $\lambda_i<0$ at $\alpha\to 2$ it is always possible to satisfy the condition $|\mathrm{Arg}(\lambda_i)|<\alpha\pi/2$, and the system becomes unstable according to homogeneous oscillations (Fig. 1(b)). The smaller is the value of tr F, the easier it is to fulfill the instability conditions.

In contrast to this case, a complex values of λ_i, with Re $\lambda_i>0$ lead to the system instability for regular system with $\alpha=1$. However, fractional derivatives with $\alpha<1$ can stabilize the system if $\alpha<\alpha_0=(2/\pi)|\mathrm{Arg}(\lambda_i)|$. This makes it possible to conclude that fractional differential equations with $\alpha<1$ are more stable than their integer twinges.

3. Solutions of the coupled fractional ordinary differential equations (FODEs)

Let us first consider the coupled FODEs which can be obtained from (1), (2) at $l=L=0$ and analyze the stability conditions for such systems. The plot of isoclines for this model is represented in Fig. 2(a). In this case homogeneous solution can be determined from the system of equations $W=Q=0$ and is given by the solution of cubic algebraic equation

$$(\beta-1)\overline{n}_1+\overline{n}_1^3/3+\mathscr{A}=0. \tag{11}$$

Simple calculation makes it possible to write useful expressions required for our analysis

$$F=-\begin{pmatrix}(-1+\overline{n}_1^2)/\tau_1 & 1/\tau_1\\ -\beta/\tau_2 & 1/\tau_2\end{pmatrix},\quad \mathrm{tr}\,F=\frac{(1-\overline{n}_1^2)}{\tau_1}-\frac{1}{\tau_2},\quad \det F=\frac{(\beta-1)+\overline{n}_1^2}{\tau_1\tau_2}.$$

It is easy to see that if the value of τ_1/τ_2, in certain cases, is less than 1, the instability conditions (tr $F>0$) lead to Hopf bifurcation for regular system ($\alpha=1$) [23,3,21,13,4]. In this case, the plot of the domain, where instability

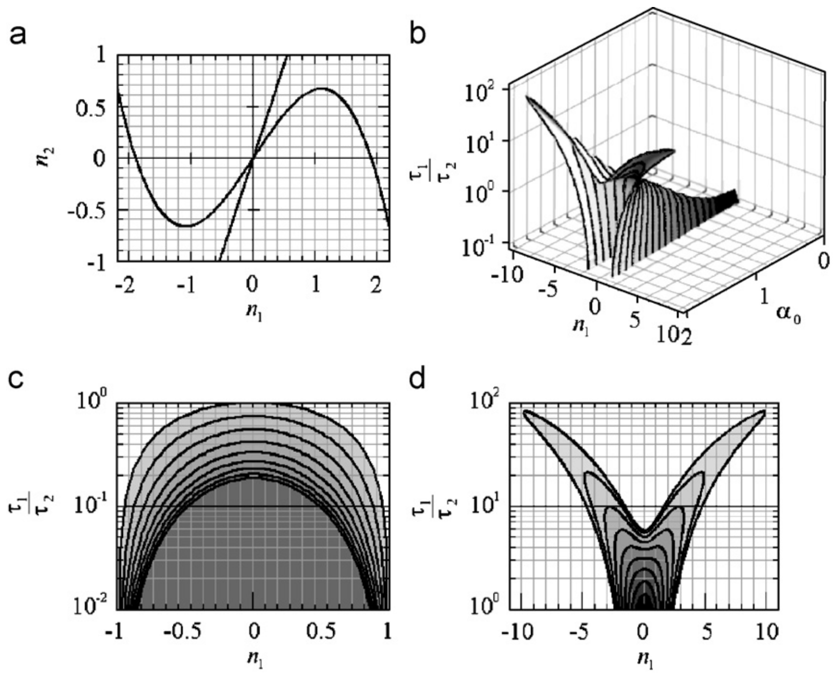

Fig. 2. Null isoclines (a), three-dimensional instability domains in coordinates $(\alpha_0,\overline{n}_1,\tau_1/\tau_2)$ (b), dependence of τ_1/τ_2 on $\overline{n}_1$ at α_0 changing from 0.1 (bottom curve) to 1.0 (upper curve) with step 0.1 (c), dependence of τ_1/τ_2 on $\overline{n}_1$ at α_0 changing from 1.1 (bottom curve) to 1.9 (upper curve) with step 0.1 (d). The shaded domains correspond to those one obtained by slicing three-dimensional surface represented in figure (b).

exists, is shown in Fig. 2(c) (unstable domain is below the upper curve). The linear analysis of the system for $\alpha = 1$ shows that, if $\tau_1/\tau_2 > 1$, the solution corresponding to the intersections of two isoclines is stable. The smaller is the ratio of τ_1/τ_2, the wider is the instability region. Formally, at $\tau_1/\tau_2 \to 0$, the instability region in $\overline{n}_1$ coincides with the interval $(-1, 1)$ where the null isocline $W(n_1, n_2) = 0$ has its increasing part. These results are very widely known in the theory of nonlinear dynamical systems [23,3,21,13,4].

In the FODEs the conditions of the instability (9) change, and we have to analyze the real and the imaginary part of the existing complex eigenvalues, especially the equation

$$4\det F - \mathrm{tr}^2 F = 4((\beta - 1) + \overline{n}_1^2)/\tau_1\tau_2 - ((1 - \overline{n}_1^2)/\tau_1 - 1/\tau_2)^2 > 0. \tag{12}$$

In fact, with the complex eigenvalues, it is possible to find out the corresponding value of α where the condition (9) is true. We will show that this interval is not correlated with the increasing part of the null isocline of the system. Indeed, omitting simple calculation, we can write an equation for marginal values of $\overline{n}_1$

$$\overline{n}_1^4 - 2\left(1 + \frac{\tau_1}{\tau_2}\right)\overline{n}_1^2 + \frac{\tau_1^2}{\tau_2^2} - 2\frac{\tau_1}{\tau_2}(2\beta - 1) + 1 = 0 \tag{13}$$

and solution of this bi-quadratic equation gives the domain where the oscillatory instability arises:

$$\overline{n}_1^2 = 1 + \frac{\tau_1}{\tau_2} \pm 2\sqrt{\beta\frac{\tau_1}{\tau_2}}. \tag{14}$$

This expression estimates the maximum and minimum values of $\overline{n}_1$ where the system can be unstable at certain value of $\alpha = \alpha_0$ as a function of τ_1/τ_2. In Fig. 2 the dependence τ_1/τ_2 is given as a function of $\overline{n}_1$ for different values of α changing with the step 0.1.

In fact, examine the domain of the FODEs where the eigenvalues are complex. The condition (9) determine dependence among values $\overline{n}_1$, τ_1/τ_2 and α_0 (this dependence is represented in Fig. 2(b)). In Fig. 2(c) and (d) cross-sections of this figure is presented for fixed value of α_0. Inside the curve system of FODEs is unstable and outside it is stable. We can see that at $\alpha < \alpha_0$ instability domain in coordinates $(\overline{n}_1, \tau_1/\tau_2)$ is smaller than for the case $\alpha_0 = 1$ (Fig. 2(c)). At the same time for the case $\alpha > \alpha_0$ instability domain increases, and the greater the value of τ_1/τ_2, the wider the region in $\overline{n}_1$ where the instability holds true (Fig. 2(d)). In this case, from (14) we immediately obtain approximate dependence ($\overline{n}_1 \simeq \pm\sqrt{\tau_1/\tau_2}$). Of course, at $\tau_1/\tau_2, \overline{n}_1 \gg 1$the interval in $\overline{n}_1$ where the instability arises increases but the domain decreases and gets the form of a narrow concave stripe following parabola $\tau_1/\tau_2 \simeq \overline{n}_1^2$ for $2 - \alpha_0 \ll 1$.

Finally, we can conclude that for $\tau_1/\tau_2 > 1$ in contrast to the regular system with integer index α fractional differential equations can be both stable and unstable. The greater the value of τ_1/τ_2, the wider the interval in $\overline{n}_1$ where instability conditions are true. Opposite situation is for $\alpha < 1$ while regular system with integer index is always unstable fractional dynamical system can be stable. It is a statement, that FODEs are at least as stable as their integer order counterparts [26]. It is obvious that this statement is true for $\alpha < 1$ only.

It should be noted that, even if the eigenvalues are not complex ($\lambda_{\mathrm{Im}} = 0$), the systems with fractional derivatives can posses oscillatory damping oscillations. Such a situation takes place when $4\det F - \mathrm{tr}^2 F < 0$, $\mathrm{tr}\, F < 0$, $\det F > 0$ and two eigenvalues are real and less than zero. In this case, at $1 < \alpha < 2$ steady-state solutions of the system are stable and any perturbations are damping. Such a system was considered, for example, in the article [37], where an analytical solution for fractional oscillator is obtained.

Our task here is to confirm our linear analysis by finding out not only the conditions of the bifurcation but also the real time dynamics of FODEs by corresponding combination of the parameters $\tau_1/\tau_2, \overline{n}_1$ for different values of $\alpha : 0 < \alpha < 2$. We have established here that the dynamics of the FODEs can be much more complicated than that one of the equations with integer order [18,6,34].

Fig. 3 gives the results of computer simulation of fractional ODEs for different cases considered above. We single out two different cases $\alpha < 1$ and $\alpha > 1$. The characteristic instability domain (shaded region) for these two cases located on the first row in two columns. Outside the shaded region system is stable and solution is given by Eq. (5). For any point inside shaded region system is unstable and we investigate nonlinear dynamics by computer simulation of the FODEs. We present nonlinear dynamics for several points denoted by capital letters A, B, C, D, E corresponding to homogeneous distributions in these points (null isoclines intersect in these points). For the points A and B taken from

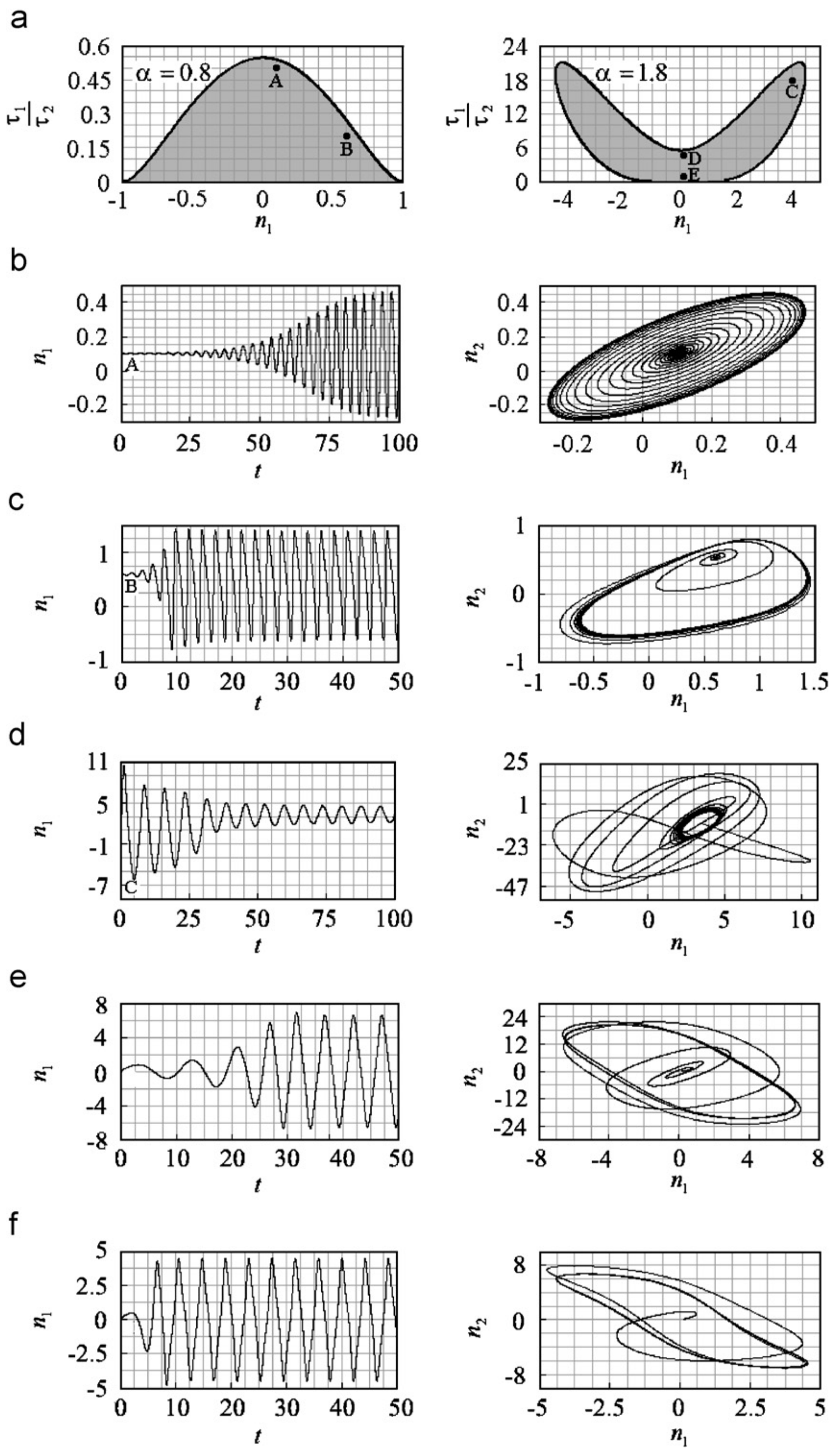

Fig. 3. Instability domains for $\alpha = 0.8$ and 1.8 (a). The time domain oscillations (left) and corresponding two-dimensional phase portrait (right) for point A (b), B (c), C (d), D (e), E (f) ($\tau_2 = 1$, $\beta = 2$, $l = L = 0$). For each point A, B, C, D and E parameter $\mathscr{A}$ corresponds to steady-state solution taken in these points.

the certain domain obtained at $\alpha = 0.8$ and for points C, D, E taken from the instability domain obtained at $\alpha = 1.8$ nonlinear dynamics is presented in Fig. 3(b)–(f).

From Fig. 3, we can see that at point A the increment of the oscillations is small enough and the formation of the limit cycle takes place during the long period ($t \simeq 100$). At the point B oscillations develop more rapidly and have a greater amplitude. The result of computer simulation of the system with $\tau_1/\tau_2 > 1$ is represented in points C, D, E. In this case in point C oscillations have a small amplitude and sufficiently large transient time. At points D and E the oscillations become fast enough and have a large amplitude.

We presented simulation of the evolutionary dynamics for only two values of indices α. Nevertheless, similar dynamics is inherent to any value of α (we investigated the α from $\alpha = 0.1$ till $\alpha = 1.9$ with step 0.1).

4. Computer simulation of pattern formation

This section contains a discussion of the results of the numerical study of system (1), (2). The system with corresponding initial and boundary conditions was integrated numerically using the explicit and implicit schemes with respect to time and centered difference approximation for spatial derivatives. The fractional derivatives were approximated using the scheme on the basis of Grünwald–Letnikov definition for $0 < \alpha < 2$ [2,26]. In fact, according to fractional calculus [26,1] between the Caputo and the Riemann–Liouville derivatives we have next relation

$$ {}_0^C D_\tau^\alpha u(\tau, \bullet) = {}_0^{\mathrm{RL}} D_\tau^\alpha u(\tau, \bullet) - \sum_{p=0}^{m} \frac{(\tau)^{p-\alpha}}{\Gamma(p-\alpha+1)} \frac{\partial^p}{\partial \tau^p} u(0^+, \bullet), \tag{15} $$

where the operator in the Riemann–Liouville sense ${}_0^{\mathrm{RL}} D_\tau^\alpha u(\tau, \bullet)$ is equivalent to the Grünwald–Letnikov operator ${}_0^{\mathrm{GL}} D_\tau^\alpha u(\tau, \bullet)$ [26,25]

$$ {}_0^{\mathrm{RL}} D_\tau^\alpha u(\tau, \bullet) = {}_0^{\mathrm{GL}} D_\tau^\alpha u(\tau, \bullet) = \lim_{\Delta t \to 0} (\Delta t)^{-\alpha} \sum_{j=0}^{[\tau/\Delta t]} (-1)^j \binom{\alpha}{j} u(\tau - j\Delta t, \bullet). $$

Because of the Grünwald–Letnikov operator is more flexible for numerical calculations and can be approximated on the interval $[0, \tau]$ with sub-interval Δt as

$$ {}_0^{\mathrm{GL}} D_\tau^\alpha u(\tau, \bullet) \approx \sum_{j=0}^{[\tau/\Delta t]} c_j^{(\alpha)} u(\tau - j\Delta t, \bullet), \tag{16} $$

where $c_j^{(\alpha)} = (\Delta t)^{-\alpha}(-1)^j \binom{\alpha}{j}$ are Grünwald–Letnikov coefficients [2,26], we used approximation (15) for our computer simulation. I should be noted that solution of the system using Grünwald–Letnikov derivative approximation (16) instead of Caputo one leads practically to the same attractor. The only difference is contained in transition dynamics due to the influence of the last term in Eq. (15). The solutions can have a different attractors at the marginal values of α when a small variations of α may change the dynamics of the system drastically.

The system of n fractional RD equations can be represented as

$$ \tau_j \frac{{}^C\partial^{\alpha_j} u_j(x,t)}{\partial t^{\alpha_j}} = d_j \frac{\partial^2 u_j(x,t)}{\partial x^2} + f_j(u_1, \ldots, u_n), \quad j = \overline{1, n}, \tag{17} $$

where τ_j, d_j, f_j are certain parameters and nonlinearities of the RD system correspondingly, the scheme can be represented as

$$ \begin{aligned} u_{j,i}^k - \frac{d_j (\Delta t)^{\alpha_j}}{\tau_j (\Delta x)^2} (u_{j,i-1}^k - 2u_{j,i}^k + u_{j,i+1}^k) - \frac{(\Delta t)^{\alpha_j}}{\tau_j} f_j(u_{1,i}^k, \ldots, u_{n,i}^k) \\ = (\Delta t)^{\alpha_j} \sum_{p=0}^{m} \frac{(k\Delta t)^{p-\alpha_j}}{\Gamma(p-\alpha_j+1)} \frac{\partial^p}{\partial t^p} u_{j,i}^0 - \sum_{l=1}^{k} c_l^{(\alpha_j)} u_{j,i}^{k-l}, \end{aligned} $$

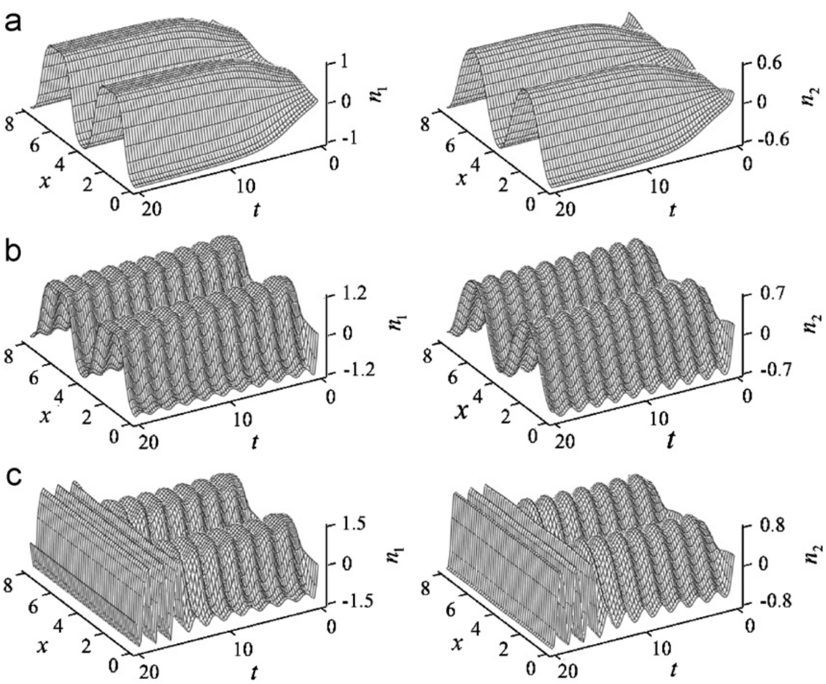

Fig. 4. Numerical solution of the fractional reaction–diffusion equations (1), (2). Dynamics of variable n_1 (left column) and n_2 (right column) on the time interval (0, 20) for $\alpha = 0.8$, $l_x = 8$, $\mathscr{A} = -0.1$, $\beta = 2$, $\tau_2 = 1$, $l^2 = 0.05$, $L^2 = 1$; $\tau_1/\tau_2 = 0.75$ (a), $\tau_1/\tau_2 = 0.15$ (b), $\tau_1/\tau_2 = 0.14$ (c). Initial conditions are $n_1^0 = \bar{n}_1 - 0.05\cos(k_0 x)$, $n_2^0 = \bar{n}_2$.

$$c_0^{(\alpha_j)} = 1, \quad c_l^{(\alpha_j)} = c_{l-1}^{(\alpha_j)} \left(1 - \frac{1+\alpha_j}{l}\right), \quad l = 1, 2, \ldots,$$

where $u_{j,i}^k \equiv u_j(x_i, t_k) \equiv u_j(i\Delta x, k\Delta t)$, $m = [\alpha]$.

The applied numerical schemes are implicit, and for each time layer they are presented as the system of algebraic equations solved by Newton–Raphson technique. Such approach makes it possible to get the system of equations with band Jacobian for each node and to use the sweep method for the solution of linear algebraic equations. Calculating the values of the spatial derivatives and corresponding nonlinear terms on the previous layer, we obtained explicit schemes for integration. Despite the fact that these algorithms are quite simple, they are very sensitive to the step size and require small steps of integration. In contrast, the implicit schemes, in certain sense, are similar to the implicit Euler's method, and they have shown very good behavior at the modeling of FRD systems for different step sizes of integration, as well as for nonlinear function and order of fractional index.

We have considered here the kinetics of formation of dissipative structures for different values of α. These results are presented in Figs. 4 and 5.

The simulations were carried out for a one-dimensional system on an equidistant grid with spatial step h changing from 0.01 to 0.1 and time step Δt changing from 0.001 to 0.1. We used Neumann (3) or periodic boundary conditions (4). As the initial condition, we used the uniform state which was superposed with a small spatially inhomogeneous perturbation.

It is very well known that in the case of $\alpha = 1$ at $l/L \ll 1$, tr $F < 0$, det $F < 0$ the homogeneous distribution (5) is unstable according to wave number [23,3,21,13,4,5,16,9,30,22]

$$k = k_0 = (a_{11}a_{22} - a_{12}a_{21})^{1/4}(Ll)^{-1/2}.$$

As a result at certain parameter $\mathscr{A}$ such that $\bar{n}_1 \in (-1, 1)$ the system can be unstable and the steady-state solutions in the form of nonhomogeneous dissipative structures arise. Such type systems have rich dynamics, including steady-state

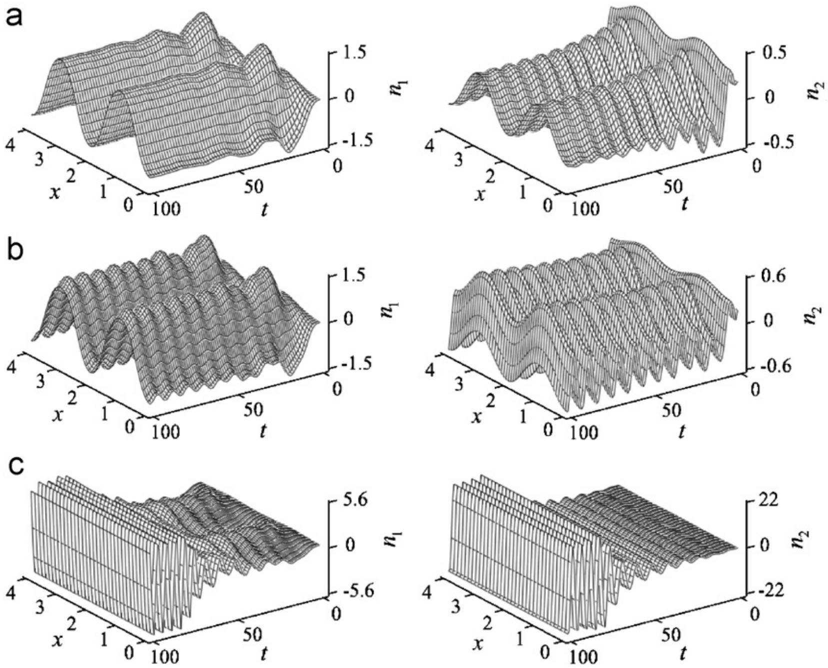

Fig. 5. Numerical solution of the fractional reaction–diffusion equations (1), (2). Dynamics of variable n_1 (left column) and n_2 (right column) on the time interval (0, 100) for $\alpha = 1.8$, $l_x = 4$, $\mathscr{A} = -0.1$, $\beta = 2$, $\tau_2 = 1$, $l^2 = 0.05$, $L^2 = 1$; $\tau_1/\tau_2 = 7$ (a), $\tau_1/\tau_2 = 6.5$ (b), $\tau_1/\tau_2 = 5.6$ (c). Initial conditions are $n_1^0 = \bar{n}_1 - 0.05\cos(k_0 x)$, $n_2^0 = \bar{n}_2$.

dissipative structures, homogeneous and nonhomogeneous oscillations, and spatio-temporal patterns. In this paper, we focus mainly on the study of general properties of the solutions depending on the value of α and the ratio of the characteristic times τ_1/τ_2.

Fig. 4(a)–(c) shows evolution of the dissipative structure formation for $\alpha < 1$. At certain values of τ_1/τ_2 we have steady-state solution (a), then with decreasing ratio of τ_1/τ_2 nonhomogeneous pulsating structures (b) and transformation of this oscillating regime to homogeneous oscillations (c).

The evolutionary dynamics for $\alpha > 1$ as the value of τ_1/τ_2 decreases is shown in Fig. 5(a)–(c). First plot corresponds to the steady-state structures (a) which start to oscillate at smaller ratio of characteristic times and eventually homogeneous oscillation are taking place in FRD system (c). Such behavior is due to the case that the oscillatory perturbations are damping in the first situation, and then small oscillations are steady state. With the further decreasing of the value τ_1/τ_2 the steady-state oscillations are unstable and dynamics changes to the homogeneous temporary behavior (Fig. 5(c)).

The emergence of homogeneous oscillations, which destroy pattern formation (Fig. 5(a)–(c)) has deep physical meaning. The matter is that the stationary dissipative structures consist of smooth and sharp regions of variable n_1, and the smooth shape of n_2. The linear system analysis shows that the homogeneous distribution of the variables is unstable according to oscillatory perturbations inside the wide interval of $\bar{n}_1$, which is much wider than interval $(-1, 1)$. At the same time, smooth distributions at the maximum and minimum values of n_1 are $\pm\sqrt{3}$ correspondingly. In the first approximation, these smooth regions of the dissipative structures resemble homogeneous ones and are located inside the instability regions. As a result, the unstable fluctuations lead to homogeneous oscillations, and the dissipative structures destroy themselves. We can conclude that oscillatory modes in such type FODEs have a much wider attraction region than the corresponding region of the dissipative structures.

It should be noted that the pulsation phenomena of the dissipative structures is closely related to the oscillation solutions of the ODE (Fig. 3). Moreover, the fractional derivative of the first variable has the most impact on the oscillations emergence. It can be obtained by performing a simulation where the first variable is a fractional derivative and the second one is an integer.

5. Conclusion

In this article we consider possible solutions of RDS with fractional derivatives. Special attention is paid to FODEs linear theory of instability which is analyzed in detail. It was shown that three parameters: fractional derivative index α, the ratio of the characteristic times τ_1/τ_2, and homogeneous solution $\overline{n}_1$ determine three-dimensional marginal surface. Inside this surface the system is unstable and outside it is stable. Nonlinear dynamics of FODEs is investigated by computer simulation of the characteristic examples.

By the computer simulation of the FRD systems we provided evidence that Turing pattern formation in the fractional case, at α less than a certain value, is practically the same as in the regular case scenario $\alpha = 1$. At $\alpha > \alpha_0$, the kinetics of formation becomes oscillatory. At $\alpha = \alpha_0$, the oscillatory mode arises and can lead to nonhomogeneous or homogeneous oscillations.

References

[1] in: A. Carpinteri, F. Mainardi (Eds.), Fractal and Fractional Calculus in Continuum Mechanics, Springer, Vienna, New York, 1997.
[2] M. Ciesielsky, J. Leszhynski, Numerical simulation of anomalous diffusion, CMM-2003, Poland (Reprinted in arXiv:math-ph/0309007).
[3] M.C. Cross, P.S. Hohenberg, Pattern formation outside of equilibrium, Rev. Modern Phys. 65 (1993) 851–1112.
[4] J.D. Dockery, J.P. Keener, Diffusive effects on dispersion in excitable media, SIAM J. Appl. Math. 49 (1989) 539–566.
[5] A. Doelman, T.J. Kaper, Semistrong pulse interactions in a class of coupled reaction–diffusion equations, SIAM J. Appl. Dynamical Systems 2 (1) (2003) 53–96.
[6] A.M.A. El-Sayed, Fractional differential-difference equations, J. Fractional Calculus 10 (1996) 101–106.
[7] V. Gafiychuk, B. Datsko, Pattern formation in a fractional reaction–diffusion system, Physica A 365 (2006) 300–306.
[8] V.V. Gafiychuk, B.Y. Datsko, Yu.Yu. Izmajlova, Analysis of the dissipative structures in reaction–diffusion systems with fractional derivatives, Math. Methods Phys. Mech. Fields 49 (4) (2006) 109–116 (in Ukrainian).
[9] V.V. Gafiychuk, I.A. Lubashevskii, Variational representation of the projection dynamics and random motion of highly dissipative systems, J. Math. Phys. 36 (10) (1995) 5735–5752.
[10] B.I. Henry, T.A.M. Langlands, S.L. Wearne, Turing pattern formation in fractional activator–inhibitor systems, Phys. Rev. E 72 (2005) 026101.
[11] I. Henry, S.L. Wearne, Fractional reaction–diffusion, Physica A 276 (2000) 448–455.
[12] B.I. Henry, S.L. Wearne, Existence of Turing instabilities in a two-species fractional reaction–diffusion system, SIAM J. Appl. Math. 62 (3) (2002) 870–887.
[13] B.S. Kerner, V.V. Osipov, Autosolitons, Kluwer Academic Publishers, Dordrecht, 1994.
[14] R. Kimmich, Strange kinetics, porous media, and NMR, Chem. Phys. 284 (2002) 243–285.
[15] N. Korabel, G.M. Zaslavsky, Transition to chaos in discrete nonlinear Schrodinger equation with long-range interaction, Physica A 378 (2007) 223–237.
[16] A. Lubashevskii, V.V. Gafiychuk, The projection dynamics of highly dissipative system, Phys. Rev. E 50 (1) (1994) 171–181.
[17] F. Mainardi, Yu. Luchko, G. Pagnini, The fundamental solution of the space–time fractional diffusion equation, Fractional Calculus Appl. Anal. 4 (2001) 153–191.
[18] D. Matignon, Stability results for fractional differential equations with applications to control processing, Comput. Eng. Systems Appl. 2 (1996) 963.
[19] V. Mendez, V. Ortega-Cejas, Front propagation in hyperbolic fractional reaction–diffusion equations, Phys. Rev. E 71 (2005) 057105.
[20] R. Metzler, J. Klafter, The random walk's guide to anomalous diffusion: a fractional dynamics approach, Phys. Rep. 339 (2000) 1–77.
[21] A.S. Mikhailov, Foundations of Synergetics, Springer, Berlin, 1990.
[22] C.B. Muratov, V.V. Osipov, Stability of the static spike autosolitons in the Gray–Scott model, SIAM J. Appl. Math. 62 (5) (2002) 1463–1487.
[23] G. Nicolis, I. Prigogine, Self-organization in Non-equilibrium Systems, Wiley, New York, 1977.
[24] Z.M. Odibat, N.T. Shawagfeh, Generalized Taylor's formula, Appl. Math. Comput. 186 (1) (2007) 286–293.
[25] K.D. Oldham, J. Spanier, The Fractional Calculus: Theory and Applications of Differentiation and Integration to Arbitrary Order, vol. 111, Academic Press, New York, 1974.
[26] I. Podlubny, Fractional Differential Equations, Academic Press, New York, 1999.
[27] A.I. Saichev, G.M. Zaslavsky, Fractional kinetic equations: solutions and applications, Chaos 7 (4) (1997) 753–764.
[28] S.G. Samko, A.A. Kilbas, O.I. Marichev, Fractional Integrals and Derivatives: Theory and Applications, Gordon and Breach, Newark, NJ, 1993.
[29] R.K. Saxena, A.M. Mathai, H.J. Haubold, Fractional reaction–diffusion equations, arXiv:math.CA/0604473, April 2006.
[30] P. Schutz, M. Bode, V.V. Gafiychuk, Transition from stationary to travelling localized patterns in two-dimensional reaction–diffusion system, Phys. Rev. E 52 (4) (1995) 4465–4473.
[31] K. Seki, M. Wojcik, M. Tachiya, Fractional reaction–diffusion equation, J. Chem. Phys. 119 (2003) 2165.
[32] V.E. Tarasov, G.M. Zaslavsky, Fractional dynamics of coupled oscillators with long-range interaction, Chaos 16 (2006) 023110.
[33] C. Varea, R.A. Barrio, Travelling Turing patterns with anomalous diffusion, J. Phys. Condens. Matter 16 (2004) 5081–5090.

[34] H. Weitzner, G.M. Zaslavsky, Some applications of fractional equations, Comm. Nonlinear Sci. Numer. Simulation 8 (2003) 273–281.
[35] R. Yu, H. Zhang, New function of Mittag–Leffler type and its application in the fractional diffusion-wave equation, Chaos, Solitons and Fractals 30 (2006) 946–955.
[36] G.M. Zaslavsky, Chaos, fractional kinetics, and anomalous transport, Phys. Rep. 371 (2002) 461–580.
[37] G.M. Zaslavsky, A.A. Stanislavsky, M. Edelman, Chaotic and pseudochaotic attractors of perturbed fractional oscillator, arXiv:nlin.CD/0508018, 2005.
[38] G.M. Zaslavsky, H. Weitzner, Some applications of fractional equations, E-print nlin.CD/0212024, 2002.